Genes & Diseases (2024) 11, 952–963

Available online at www.sciencedirect.com

ScienceDirect

journal homepage: www.keaipublishing.com/en/journals/genes-diseases

FULL LENGTH ARTICLE

Cellular senescence-driven transcriptional reprogramming of the *MAFB/NOTCH3* axis activates the *PI3K/AKT* pathway and promotes osteosarcoma progression

Zhenhao Zhang [a,1], Doudou Jing [b,1], Baijun Xuan [c,1], Zhicai Zhang [a,*], Wei Wu [a,*], Zengwu Shao [a,*]

[a] *Department of Orthopedics, Union Hospital, Tongji Medical College, Huazhong University of Science and Technology, Wuhan, Hubei 430022, China*
[b] *Department of Orthopedics, The Second Hospital of Shanxi Medical University, Taiyuan, Shanxi 030001, China*
[c] *Department of Cardiology, Union Hospital, Tongji Medical College, Huazhong University of Science and Technology, Wuhan, Hubei 430022, China*

Received 27 July 2022; accepted 8 February 2023
Available online 27 March 2023

KEYWORDS
Cellular senescence;
Elderly patients;
*MAFB-NOTCH3*axis;
Methylmalonic acid;
Osteosarcoma;
*PI3K-AKT*pathway

Abstract Osteosarcoma is the most common primary malignancy of bones and primarily occurs in adolescents and young adults. However, a second smaller peak of osteosarcoma incidence was reported in the elderly aged more than 60. Elderly patients with osteosarcoma exhibit different characteristics compared to young patients, which usually results in a poor prognosis. The mechanism underlying osteosarcoma development in elderly patients is intriguing and of significant value in clinical applications. Senescent cells can accelerate tumor progression by metabolic reprogramming. Recent research has shown that methylmalonic acid (MMA) was significantly up-regulated in the serum of older individuals and played a central role in the development of aggressive characteristics. We found that the significant accumulation of MMA in elderly patients imparted proliferative potential to osteosarcoma cells. The expression of *MAFB* was excessively up-regulated in osteosarcoma specimens and was further enhanced in response to MMA accumulation as the patient aged. Specifically, we first confirmed a novel molecular mechanism between cellular senescence and cancer, in which the MMA-driven transcriptional reprogramming of the *MAFB-NOTCH3* axis accelerated osteosarcoma progression via the activation of *PI3K-AKT* pathways. Moreover, the

* Corresponding author.
E-mail addresses: zhicaizhang@126.com (Z. Zhang), waynewu@hust.edu.cn (W. Wu), 1985xh0536@hust.edu.cn (Z. Shao).
Peer review under responsibility of Chongqing Medical University.
[1] These authors contributed equally to this work.

https://doi.org/10.1016/j.gendis.2023.02.028

down-regulation of the *MAFB-NOTCH3* axis increased the sensitivity and effect of *AKT* inhibitors in osteosarcoma through significant inhibition of *AKT* phosphorylation. In conclusion, we confirmed that *MAFB* is a novel age-dependent biomarker for osteosarcoma, and targeting the *MAFB-NOTCH3* axis in combination with *AKT* inhibition can serve as a novel therapeutic strategy for elderly patients with osteosarcoma in experimental and clinical trials.

Introduction

Osteosarcoma is the most common primary malignancy of bone and is primarily reported in adolescents and young adults.[1,2] However, a second peak of osteosarcoma incidence has been observed in elderly individuals aged more than 60 years, which is often ignored.[3,4] Traditional chemotherapy for adolescents often fails to yield the desired effect in elderly patients because of cancer onset at the spine and pelvis, distant metastasis, and resistance to chemotherapy, which leads to poor prognosis.[5] The mechanism underlying osteosarcoma in elderly patients is intriguing and of substantial value in clinical application.

A growing body of evidence indicates that senescent cells stimulate tumor development and malignant progression via varying mechanisms.[6,7] Recent studies have shown that senescent cells can accelerate tumor progression by remodeling the tumor microenvironment and altering cellular transcription patterns, which are mediated by specific metabolites.[8]

Endogenous metabolic by-products in the tumor microenvironment are not mere bystanders, but critical regulators in cancer development and carcinogenicity.[9] Methylmalonic acid (MMA), a by-product of the tricarboxylic acid cycle, is generated by removing coenzyme A from methylmalonyl-coenzyme A which mainly comes from the catabolism of branched-chain amino acids and odd-chain fatty acids.[10] Under normal physiological conditions, MMA has no specific physiological function.[10] However, methylmalonic acidemia, a congenital metabolic disease, is characterized by the accumulation of methylmalonic acid in the blood, causing acidosis and damage to multiple systems.[10] A new study has confirmed that MMA production is significantly increased in the serum of elderly individuals and promotes invasiveness of triple-negative breast cancer and non-small cell lung cancer.[8] However, to date, no study has been conducted on the specific functions of MMA in other cancers.

The members of MAF bZIP transcription factor (MAF) family, characterized by basic leucine zipper (bZIP) domains that bind to specific DNA elements,[11] include small MAF proteins (*i.e.*, MAFF, MAFG, and MAFK) and the large MAF proteins (*i.e.*, MAFA, MAFB, c-MAF, and neural retina-specific leucine zipper).[12] These were originally considered to represent the viral oncogene, encoded by avian retrovirus AS42 and isolated from a spontaneous musculoaponeurotic fibrosarcoma (MAF) in chicken.[13] These MAF proteins regulate cell differentiation[14] and the pattern of tissue-specific gene expression[15] in various tissues and participate in human tumor genesis and development.[14] *MAF bZIP* transcription factor B (MAFB) has been proven to facilitate the proliferation and migration of nasopharyngeal carcinoma cells.[16] MAFB chromosomal translocation often appears in human myeloma cells.[17] Recent studies have shown that MAFB can serve as a marker of tumor-associated macrophages.[18] However, the role of MAFB in osteosarcoma has rarely been reported.

Here, we evaluated findings from recent studies to develop hypotheses and for experimental exploration and verification of data. Cancer cells are widely known to promote their survival and increase carcinogenicity through the reprogramming of their biochemical pathways.[19] Interestingly, we found that cancer cells can modulate transcription patterns by directly using the metabolic characteristics of senescence. In our study, the serum MMA concentration increased significantly and up-regulated *MAFB* expression in tumor tissue specimens collected from elderly osteosarcoma patients. Moreover, we confirmed the critical roles of the *MAFB-NOTCH3* axis on osteosarcoma and revealed a type of internal molecular mechanism between cellular senescence and tumor progression.

Materials and methods

The human serum and tissue specimens

Twenty patients with osteosarcoma who were diagnosed in the Department of Orthopedics, Union Hospital, Tongji Medical College, Huazhong University of Science and Technology, Wuhan, from January 2020 to January 2022, were selected. The human blood of twelve "young" (25 years old and below) and eight "old" (45 years old and above) osteosarcoma patients were centrifuged immediately after collection at different times and stored at −80 °C. The information on the human serum used in this study is shown in Table S1. Eight sera samples, including four samples from young donors and four samples from old donors, were selected from these sera specimens to treat with osteosarcoma cells. The detailed information is shown in Table S2. Six samples, including three young patients' specimens and three old patients' specimens, were selected from these twenty tissue specimens to detect the

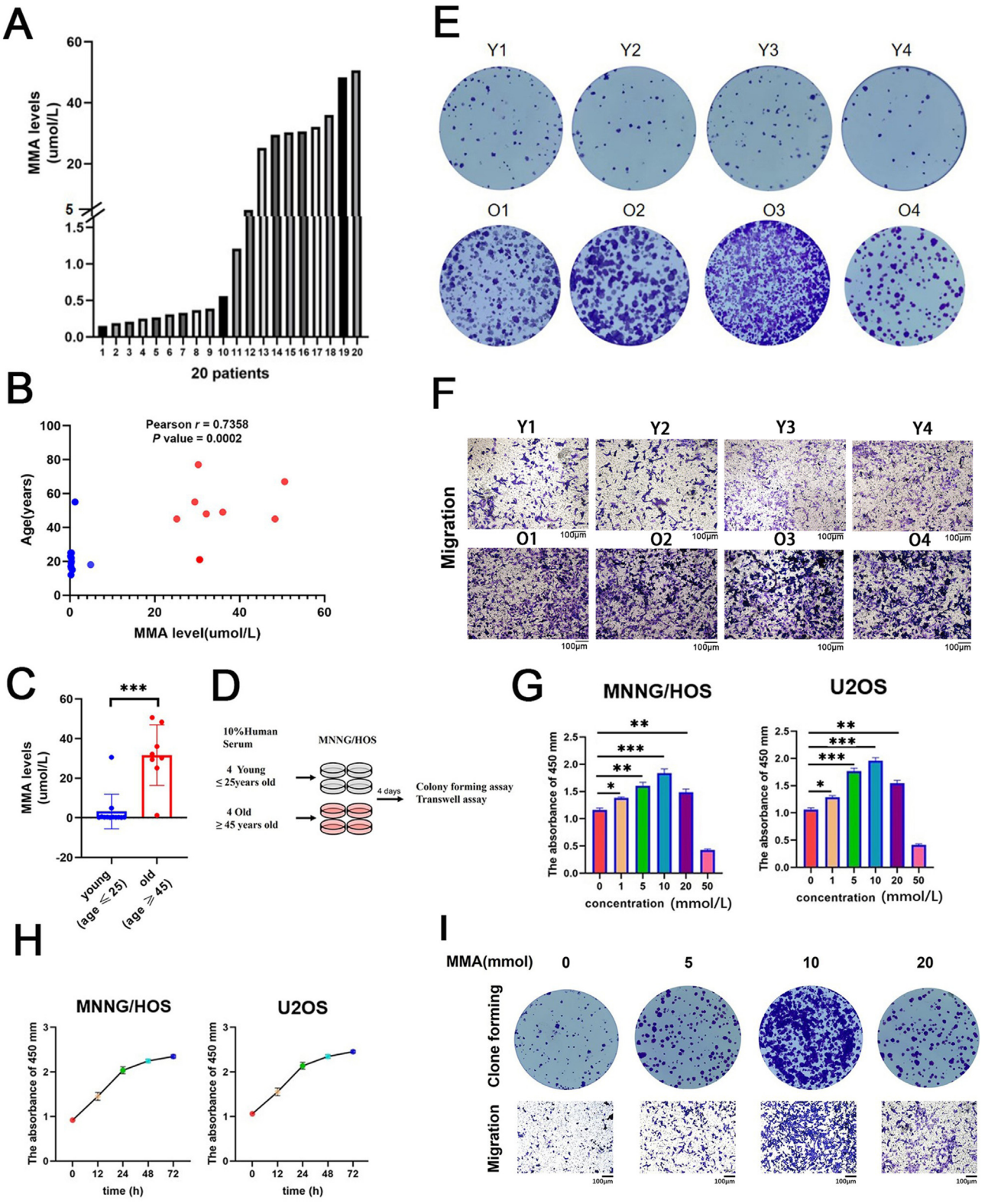

Figure 1 MMA accumulates in the serum of elderly patients with osteosarcoma and accelerates cancer progression. **(A)** The serum MMA concentrations in osteosarcoma specimens collected from elderly patients were measured using an MMA Elisa assay kit according to the manufacturer's instructions (FT-P36871R, Fan Tai Bio). Table S1 shows the detailed data. **(B)** Correlation analysis of the serum MMA level with age was determined using Pearson's *r*. Pearson's $r = 0.7358$, *P* value $= 0.0002$. The red plots represent old patients (age $\geq$45 years), and the blue plots represent young patients (age $\leq$25 years old). **(C)** A two-sided paired Student's *t*-test was used to analyze the difference in serum MMA levels between young and old patients. Data were presented as the mean $\pm$ standard deviation (SD) of three independent experiments. ***$P < 0.001$. **(D)** Flow diagram for the treatment of MNNG/HOS

mRNA and protein expression of *MAFB*. Detailed information on the six patients is shown in Table S3.

Measurements of MMA concentrations in human sera

Determination of the serum MMA concentrations was conducted by MMA Elisa assay kit according to the manufacturer's protocol (FT-P36871R, Fan Tai Bio). Briefly, after the blood from patients was coagulated at room temperature, the upper sera were collected by centrifugation. The sera were added to the antibody-coated enzyme label plate, and then horseradish peroxide was added. The mixture was incubated at 37 °C for 60 min. After the immune complex was formed, the residual components were washed away, followed by the addition of a chromogenic substrate (3,3′,5,5′-tetramethylbenzidine, TMB) and 15 min later the termination solution to terminate the reaction. The optical density (OD) value was measured at the wavelength of 450 nm using a microplate reader, and the concentration of MMA in the samples was calculated by drawing a standard curve. The raw data details of the MMA detection result in this study are shown in Table S1.

Immunohistochemistry (IHC)

Samples from 20 patients were stained via the EnVision two-step immunohistochemical technique, using a Leica Benchmark-ULTRA Autostainer for *MAFB* antigens. The subcellular location of MAFB is mainly in the nucleus, but a small part is still located in the plasma membrane, Golgi apparatus, lysosome, endoplasmic reticulum, and mitochondrion. IHC analysis was performed to detect the protein expression level with the *MAFB* antibody (Cell Signaling Technology, #30919 S, 1:200). Two independent pathologists, who were unknown of the patient clinical information and histopathological features of the samples, were responsible for reviewing and scoring the degree of immunostaining separately. Human normal muscle tissue was selected to perform the same immunohistochemical protocol and was used as a negative control. Similarly, osteosarcoma tissue was acquired from the nude mice model to perform the same immunohistochemical protocol for staining Ki-67. The patients' details of immunohistochemistry specimens used in this study are shown in Table S1.

Immunocytochemistry (ICC) and immunofluorescence (IF)

The cells implanted in 48 well plates were washed and added with 4% paraformaldehyde fixation solution and fixed at room temperature for 30 min. After washing, 0.1% Triton X-100 was added to the cells for cell lysis at room temperature for 15 min. After washing, the samples were blocked with 5% goat serum and incubated at 37 °C for 2 h. After discarding the blocking solution, the diluted corresponding primary antibody was added to the sample for incubation overnight at 4 °C. After washing, diluted fluorescent-labeled secondary antibody was added to the sample for 1-h incubation at 37 °C in dark. After washing, the nuclei were labeled with DAPI stain and reacted at room temperature without light for 15 min. After washing, the wells were photographed by fluorescence multichannel with an Olympus IX70 inverted microscope in dark. At most 5 random 200× microscopic visual fields were selected randomly in per well. The experiment in each group was repeated at least three times.

Chromatin immunoprecipitation (ChIP)-PCR assay

ChIP assays were carried out according to the manufacturer's protocol (#9005s, Cell Signaling). Briefly, we collected osteosarcoma cells and added formaldehyde to cells in PBS buffer to configure the final concentration as 1%. After eliminating the supernatant of samples, the cell debris mixture was sonicated to cleave DNA fragments to 100—900 bp. After immunoprecipitation by the corresponding antibody, the chromosomes were eluted from the protein *G* microspheres and de-crosslinked. Then DNA samples were purified through spin purification columns. Finally, a PCR assay was used for ChIP enrichment efficiency analysis. The enrichment results of specific DNA regions were normalized by respective control IgG values. The primer sequences of genes used in this study are listed in Table S4.

In vivo assay

All the animal experimental protocols were authorized by the Ethics Committee of Tongji Medical College, Huazhong University of Science and Technology. 5×10^6 MNNG/HOS cells were injected hypodermically into the right flank of nude mice (BALB/c, female, 4—5 weeks old, 18—20 g). All mice were randomly divided into three groups ($n = 5$ per group) and the cells for injection were treated differently. Normal saline solution or MK2206 (120 mg/kg/days) was intraperitoneally injected into the mice. MNNG/HOS cells were treated with 10 mM MMA for 3 days, which was added with HEPES buffer to modulate PH to 7.4. The mice implanted with MMA-treated cells were treated for 16 days with MMA (200 μg MMA/g/days) by subcutaneous injection during the experiment. The volume of the grafts was measured every other day. Tumor volumes were calculated using the following formula: tumor volume (mm^3) =

cells with patient sera. **(E)** Colony-forming assay for MNNG/HOS cells treated with patient sera. Four samples were collected each from the young group (Y1, Y2, Y3, and Y4) and the old group (O1, O2, O3, O4). **(F)** Transwell assay was used to test the migration potential of MNNG/HOS cells. The groups were determined as mentioned above. $n = 3$. **(G, H)** The viability of MNNG/HOS and U2OS cells was determined using the CCK8 assay. Cells were treated with 0, 1, 5, 10, 20, or 50 mmol/L MMA (G). Cells were treated with 10 mmol/L MMA and detected at 0, 12, 24, 48, and 72 h after treatment (H). Subsequent mentions of "MMA treatment" refer to "treatment with 10 mmol/L MMA for 24 h". Data were presented as the mean ± SD. $^*P < 0.05$; $^{**}P < 0.01$; $^{***}P < 0.001$; $n = 3$. **(I)** Cell proliferation was detected in the colony-forming assay. Cell migration was measured using the Transwell assay. MNNG/HOS and U2OS cells were pre-treated with 0, 5, 10, or 20 mmol/L MMA. $n = 3$.

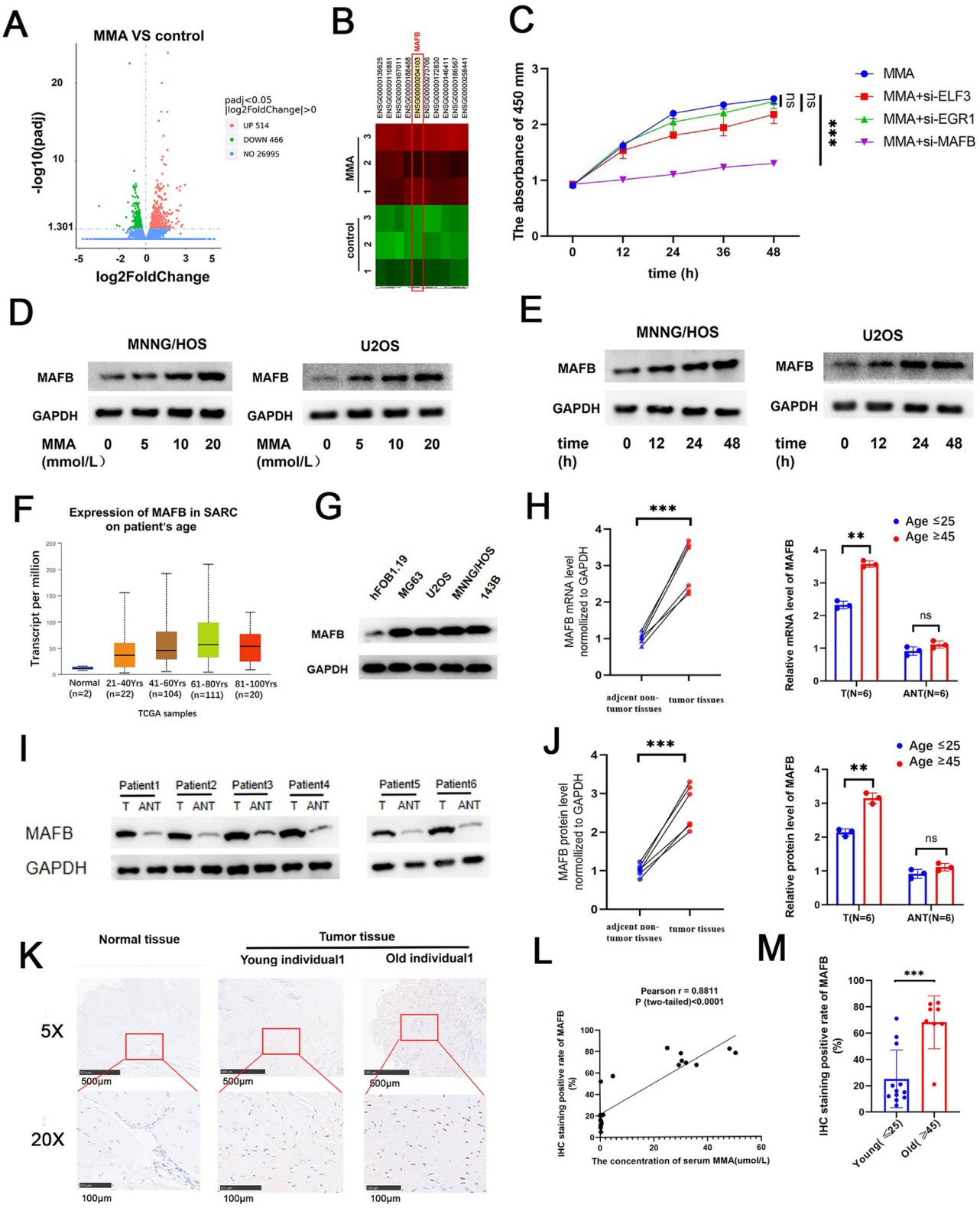

Figure 2 MAFB is overexpressed in osteosarcoma and its excessive up-regulation is induced by MMA. **(A, B)** RNA sequencing analysis results shown in the volcano plot (A) and heatmap (B) indicated the presence of 980 differentially expressed genes in MNNG/HOS cells treated with or without MMA. **(C)** Cell viability was determined using the CCK8 assay. MNNG/HOS cells were transfected with specific si-RNA and observed at 0, 12, 24, 36, and 48 h after MMA treatment. Data were presented as the mean ± standard deviation (SD) of three independent experiments. ns, not significant; ***$P < 0.001$; $n = 3$. **(D, E)** *MAFB* expression in MNNG/HOS and U2OS cells was detected using Western blot analysis. Cells were treated with 0, 5, 10, or 20 mmol/L MMA and detected after 24 h (D). Cells were treated with 10 mmol/L MMA and detected at 0, 12, 24, and 48 h after treatment (E). **(F)** *MAFB*

$(L \times W^2) \div 2$. Mice were sacrificed on day 21 or when tumor volume reached 1000 mm^3. The mass of the grafts was calculated from standard measurements.

Statistical analysis

Data were expressed as mean ± standard deviation (SD) of at least three independent experiments. GraphPad Prism 8 software (GradPad Software, Inc.) was used for all statistical analyses. Statistical analyses were performed using one- or two-sided paired Student's *t*-test for single comparison and one- or two-way ANOVA with a posthoc test for multiple comparisons, and the results were considered significant at $P < 0.05$.

Image *J* was used to conduct colocalization analysis for the result of ICC and IF. Pearson *r* was used to measure the linear correlation between variables. It measures the linear correlation between variables. Its value is less than or equal to 1 and greater than or equal to −1. Its absolute value indicates the degree of correlation between the two variables. If it was equal to 0, it indicated no correlation; if it was more than 0, it indicated a positive correlation; if it was less than zero, it indicated a negative correlation.

Results

MMA accumulates in the serum of elderly patients with osteosarcoma and accelerates cancer progression

Considering that osteosarcoma had the second peak incidence in the elderly,[3,4] we evaluated findings from the existing study on the relationship between MMA levels and "old" age.[8] Thus, we hypothesized that the systematic accumulation of MMA caused by cellular senescence would accelerate osteosarcoma progression. First, we measured the serum MMA levels of 20 patients with osteosarcoma in our clinical specimen repository (Fig. 1A) and found that the level of MMA in elderly patients was significantly higher than that in young patients (Fig. 1A, B) (Table S1 shows the data collected from 20 patients). Second, we cultured MNNG/HOS cells in 10% human serum from four young (age ≤25 years) and four old (age ≥45 years) patients with osteosarcoma (Fig. 1D) (Table S2 shows the donor information of the four patients). MNNG/HOS cells cultured with the old donor serum showed significantly higher levels of osteosarcoma cell proliferation and migration (Fig. 1E, F). Exogenous MMA reagent exerted an effect on osteosarcoma that was like the effect observed with aged sera with a higher MMA concentration. The MMA reagent enhanced the viability of osteosarcoma cells in a dose- and time-dependent manner (Fig. 1G, H). Similarly, the results of the clone forming and Transwell assays showed that MMA significantly promoted cell proliferation and migration in osteosarcoma (Fig. 1I). Thus, our data showed that MMA accumulation caused by cellular senescence-accelerated cancer progression and endowed osteosarcoma cells with proliferative potential. Nevertheless, the internal molecular mechanism underlying MMA warrants further investigation.

MAFB is overexpressed in osteosarcoma and its excessive up-regulation is induced by MMA

The RNA sequencing analysis was conducted for MNNG/HOS cells treated with 10 mmol/L MMA for 2 days. A total of 980 genes showed significant changes in expression, of which 466 genes were up-regulated and 514 genes were down-regulated (Fig. 2A, B). Notably, the results of differential gene enrichment analysis showed that among the differentially expressed genes encoding transcription factors, only the *ELF3*, *EGR1*, *MAFB*, *PRDM16*, and *ZNF536* genes showed significant changes in expression. Concurrently, PCR verification was conducted using osteosarcoma cells treated with MMA. Among the five up-regulated transcription factors, *ELF3*, *EGR1*, and *MAFB* showed the most significant changes (up-regulation ≥ two times) (Fig. S1A). A small interfering RNA (siRNA)-based method was used to knock down the *ELF3*, *EGR1*, and *MAFB* genes in the MNNG/HOS and U2OS cells (Fig. S1B). Only *MAFB* knockdown significantly inhibited the positive effects of MMA in osteosarcoma cells, whereas the down-regulation of *ELF3* or *EGR1* exerted a limited effect (Fig. 2C). TCGA database showed that *MAFB* was overexpressed at the mRNA level in a variety of malignant tumors, especially in sarcoma (Fig. S1C, D). Moreover, in the TCGA database, the mRNA expression of *MAFB* significantly increased as the patient aged (Fig. 2F). Concurrently, TCGA data showed that patients with sarcoma with higher *MAFB* expression had a shorter disease-free survival time ($P = 0.0029$) (Fig. S1E). Furthermore, compared with a normal osteogenic cell line, the four osteosarcoma cell lines showed up-regulation of *MAFB* mRNA and protein expression (Fig. 2G; Fig. S1F). Similarly, the mRNA and protein expression levels of *MAFB* in osteosarcoma specimens were higher than those in adjacent normal specimens (Fig. 2H–J). Moreover, the

mRNA expression in sarcoma based on patient age determined with the TCGA data using the UALCAN web tool. Normal ($n = 2$), 21–40 years old ($n = 22$), 41–60 years old ($n = 104$), 61–80 years old ($n = 111$), and 81–100 years old ($n = 20$). **(G)** *MAFB* expression in one normal osteogenic cell line and four osteosarcoma cell lines was detected using Western blot analysis. **(H)** *MAFB* mRNA expression was detected by RT-qPCR analysis. Six pairs of T/ANT specimens from our clinical specimen bank were tested. "T" refers to tumor tissue and "ANT" refers to adjacent non-tumor tissue. Data were presented as the mean ± SD of three independent experiments. ns, not significant; $^{**}P < 0.01$; $^{***}P < 0.001$. **(I, J)** *MAFB* expression in clinical specimens was detected by Western blot analysis (I). Data were presented as the mean ± SD of three independent experiments (J). ns, not significant; $^{**}P < 0.01$; $^{***}P < 0.001$. **(K)** Immunohistochemistry results of *MAFB* staining in a part of the clinical specimens. **(L)** A two-sided paired Student's *t*-test was used to analyze the difference in the IHC staining rate of *MAFB* and serum MMA levels between the young group (age ≤25) and the old group (age ≥45). Data were presented as the mean ± SD of three independent experiments. $^{***}P < 0.001$. **(M)** Correlation analysis between the serum concentration of MMA and the IHC staining rates of *MAFB* was drawn by a scatter diagram and measured using Pearson's *r* ($r = 0.8811$) and *P* value ($P < 0.0001$).

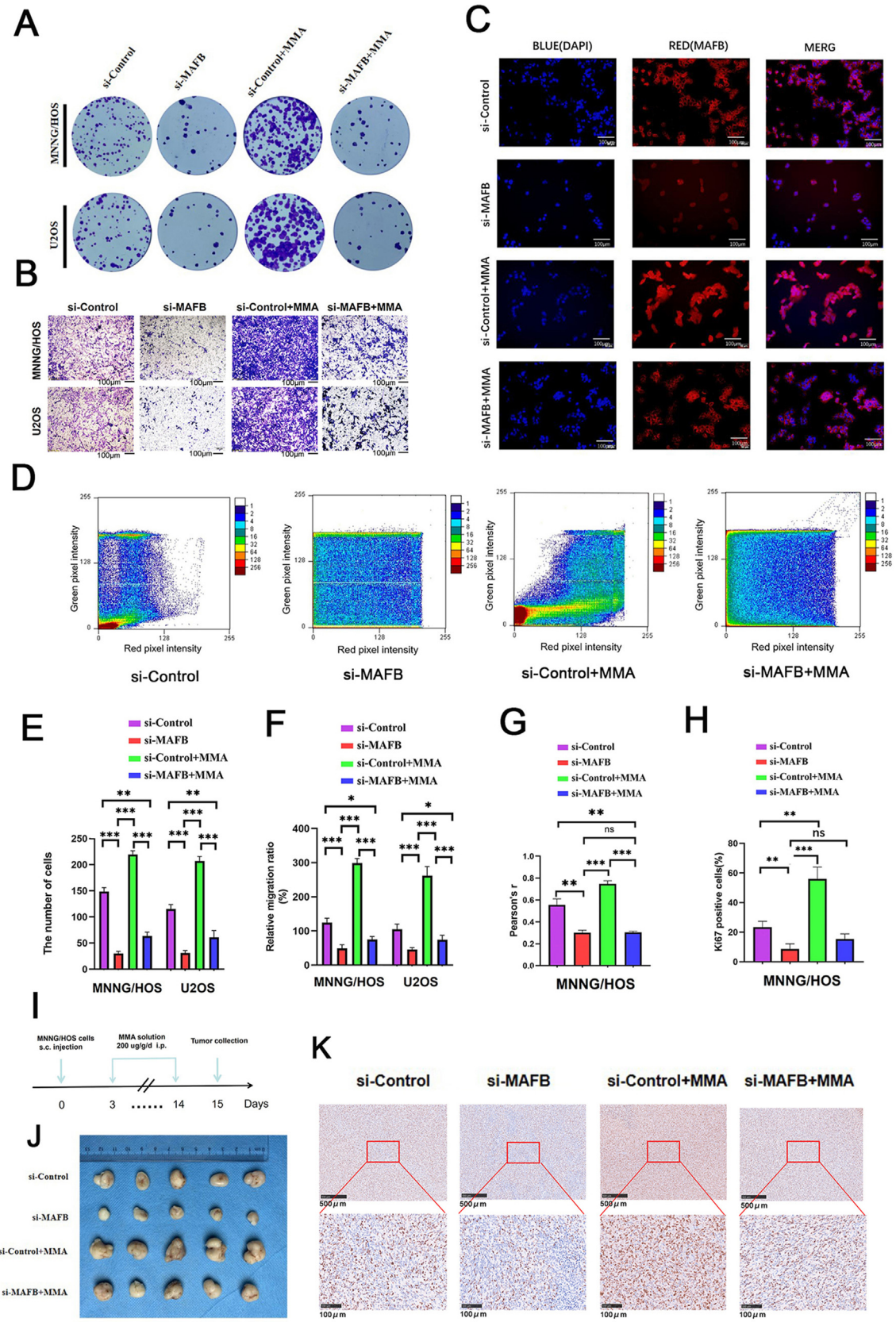

Figure 3 MAFB up-regulation promotes the proliferation and migration of osteosarcoma cells. **(A)** Cell proliferation was detected in the colony-forming assay. MNNG/HOS and U2OS cells were transfected separately with si-Control or si-*MAFB* and treated with or without MMA. **(B)** Cell migration was detected in the Transwell assay. MNNG/HOS and U2OS cells were treated separately, as described above. **(C)** MAFB expression and subcellular co-localization were detected using immunocytochemistry and

mRNA and protein expression levels of *MAFB* in osteosarcoma specimens from elderly patients were significantly higher than those in specimens from young patients (Fig. 2H—J). Next, IHC staining showed that the positive rate of *MAFB* staining in aged specimens was higher than that in young specimens (Fig. 2K, L). Furthermore, we found that the high serum level of MMA may be associated with a high positive rate of *MAFB* staining in specimens (Fig. 2M). Thus, our results showed that *MAFB* is the downstream target of MMA and is overexpressed in osteosarcoma cells at the mRNA and protein levels. Moreover, with age, the high expression of *MAFB* could be further induced by MMA. Nevertheless, the specific function and effect of *MAFB* in osteosarcoma require verification.

MAFB up-regulation promotes the proliferation and migration of osteosarcoma cells

To further explore the specific carcinogenic functions of *MAFB* in osteosarcoma, *MAFB* expression in U2OS and MNNG/HOS cells was knocked down by infection with specific siRNA (Fig. S2A). MMA treatment and *MAFB* up-regulation could significantly promote the proliferation and migration of osteosarcoma cells, and the down-regulation of *MAFB* could significantly inhibit these effects of MMA (Fig. 3A, B, E, F). *MAFB* is a specific transcription factor that primarily functions in the nucleus. The results of immunofluorescence staining in MNNG/HOS cells showed that MMA could not only increase the intracellular expression level of *MAFB* protein but also the nuclear distribution and concentration of *MAFB* (Fig. 3C, D, G). In addition, the xenograft model in nude mice showed that MMA significantly promoted tumor growth and increased the Ki-67-positive rate of cells, whereas *MAFB* knockdown reversed this process (Fig. 3H—K). Thus, our data suggested that *MAFB* expression promotes osteosarcoma proliferation *in vivo* and *in vitro*, but the specific molecular mechanism requires further verification.

MAFB promotes the transcription of *NOTCH3* through protein-DNA interactions

To further explore the downstream target of *MAFB*, 5192 downstream target genes of *MAFB* were predicted using the biological database network (Fig. 4B). Upon comparison with the mRNA sequencing results of MNNG/HOS cells treated with MMA (Figs. 4A), 11 genes with overlapping expression were identified (Fig. 4C, D). ChIP-PCR results of these genes in MNNG/HOS cells showed that the specific binding between *MAFB* protein and *NOTCH3* DNA was the most significant (Fig. 4E). Flag-tagged *MAFB* constructs were transfected into MNNG/HOS and U2OS cells (Fig. 4F). The results showed that MMA could increase the protein expression of *NOTCH3*, whereas *MAFB* silencing could inhibit the MMA-induced up-regulation of *NOTCH3*, and *MAFB* overexpression could restore the MMA-induced up-regulation of *NOTCH3* (Fig. 4G). Thus, the results showed that *MAFB* could regulate the expression of *NOTCH3* at the transcriptional level through protein-DNA interactions.

Activation of the *PI3K-AKT* pathway by the *MAFB-NOTCH3* axis promotes osteosarcoma proliferation

The RNA sequence results of MNNG/HOS cells treated with MMA were analyzed for KEGG pathway enrichment and showed that the *PI3K-AKT* signaling pathway was markedly enriched (Fig. 5A). It is universally known that the *PI3K-AKT* signaling pathway promotes proliferation and other biological behaviors in several types of cancers.[20] Western blotting confirmed that MMA increased phosphorylation in the *PI3K-AKT-mTOR* signaling pathway in osteosarcoma cells in a dose-dependent manner (Fig. 5B). We infected osteosarcoma cells with specific siRNA to induce *NOTCH3* knockdown (Fig. S3A). *MAFB* down-regulation inhibited the MMA-induced activation of *AKT* phosphorylation, whereas *NOTCH3* overexpression reversed the inhibition of *AKT* phosphorylation in response to *MAFB* down-regulation (Fig. 5C). Moreover, the level of *AKT* phosphorylation, which was lowered upon the inhibition of the *MAFB-NOTCH3* axis, declined further in response to treatment with an *AKT* inhibitor (MK2206) (Fig. 5D). The knockdown of *NOTCH3* in MNNG/HOS cells markedly reduced the IC_{50} value of MK2206 and enhanced the growth inhibitory effect of MK2206 (Fig. 5E). To explore the specific role of *NOTCH3*, we conducted clone forming and Transwell assays. Treatment with MK2206 alone could significantly attenuate the proliferation and migration potential of osteosarcoma cells, and *NOTCH3* silencing could significantly enhance these inhibitory effects of MMA (Fig. 5F, G). Similarly, compared with MK2206 treatment alone, MK2206 treatment combined with *NOTCH3* silencing in osteosarcoma cells significantly inhibited tumor growth and decreased the number of Ki-67-positive cells in the nude mice xenograft assay (Fig. 5I, J; Fig. S4B). Thus, *PI3K-AKT* pathway activation regulated by the *MAFB-NOTCH3* axis promoted osteosarcoma proliferation and migration *in vivo* and *in vitro*.

immunofluorescence assays, respectively. MNNG/HOS cells were treated separately, as described above. **(D)** Subcellular MAFB colocalization was analyzed using a scatter diagram. **(E, F)** The statistical graph of data from the colony-forming assay (E) and Transwell assay (F). Data were presented as mean ± SD. $^{*}P < 0.05$, $^{**}P < 0.01$, $^{***}P < 0.001$; $n = 3$. **(G)** Subcellular *MAFB* colocalization was measured by Pearson's *r*. The groups were formed as mentioned above. Data were presented as mean ± SD. ns, not significant; $^{*}P < 0.05$, $^{**}P < 0.01$, $^{***}P < 0.001$; $n = 3$. **(H)** Tumor tissue acquired from nude mice in the xenograft assay was used in the immunohistochemistry assay for Ki-67 staining. The groups were formed as mentioned above. Data were presented as mean ± SD of five replicates. ns, not significant; $^{*}P < 0.05$; $^{**}P < 0.01$; $^{***}P < 0.001$; $n = 5$. **(I)** Flow diagram for the xenograft assay in nude mice. **(J)** The result of the xenograft assay in nude mice. Implanted MNNG/HOS cells were transfected with si-*MAFB* or si-Control; MMA solution or PBS buffers were injected. $n = 5$. **(K)** The tumor tissue acquired from nude mice in the xenograft assay was used in the immunohistochemistry assay for Ki-67 staining. The groups were formed as mentioned above.

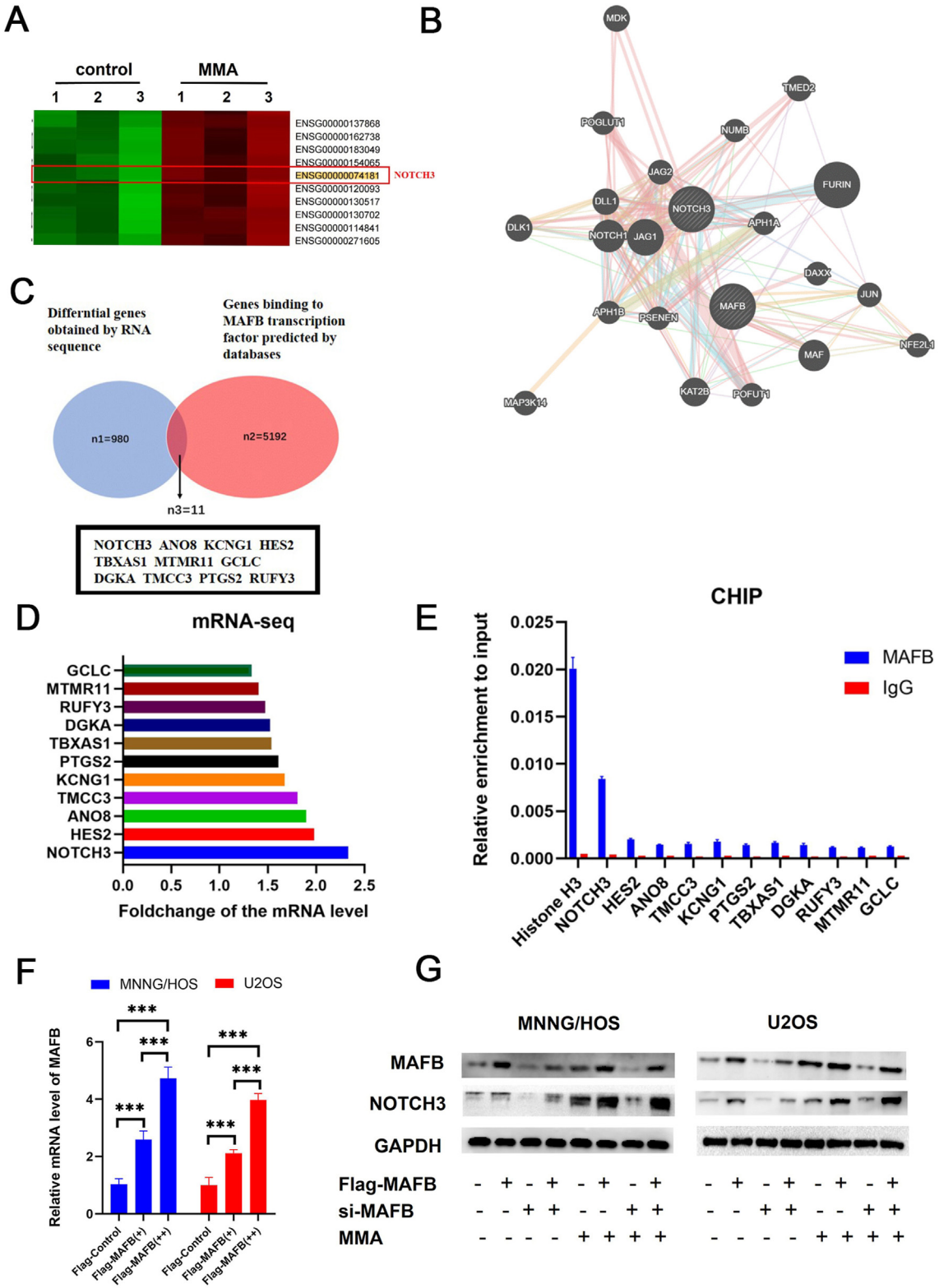

Figure 4 MAFB promotes the transcription of *NOTCH3* through protein-DNA interactions. **(A)** RNA sequencing analysis results shown in the heatmap indicate the differentially expressed genes in MNNG/HOS cells treated with or without MMA. **(B)** Downstream target genes of *MAFB* were predicted using the biological database network. **(C)** Wayne diagram showing differentially expressed genes identified by RNA sequencing and target genes of *MAFB* predicted using the Gene Transcription Regulation Database (GTRD). **(D)** mRNA expression of 11 overlapping genes based on the results of RNA sequencing. **(E)** The combination of *MAFB* protein and *NOTCH3* chromatin was detected using the ChIP assay and evaluated by relative enrichment to input. Histone H3 served as the positive control. **(F)** MNNG/HOS and U2OS cells were infected with the indicated plasmids. After 48 h, the cells were harvested for RT-qPCR analysis. **(G)** The expression of *NOTCH3* and *MAFB* was detected by Western blot analysis. MNNG/HOS or U2OS cells were transfected with Flag-*MAFB* or Flag-Control and si-*MAFB* or si-Control and treated with or without MMA, respectively.

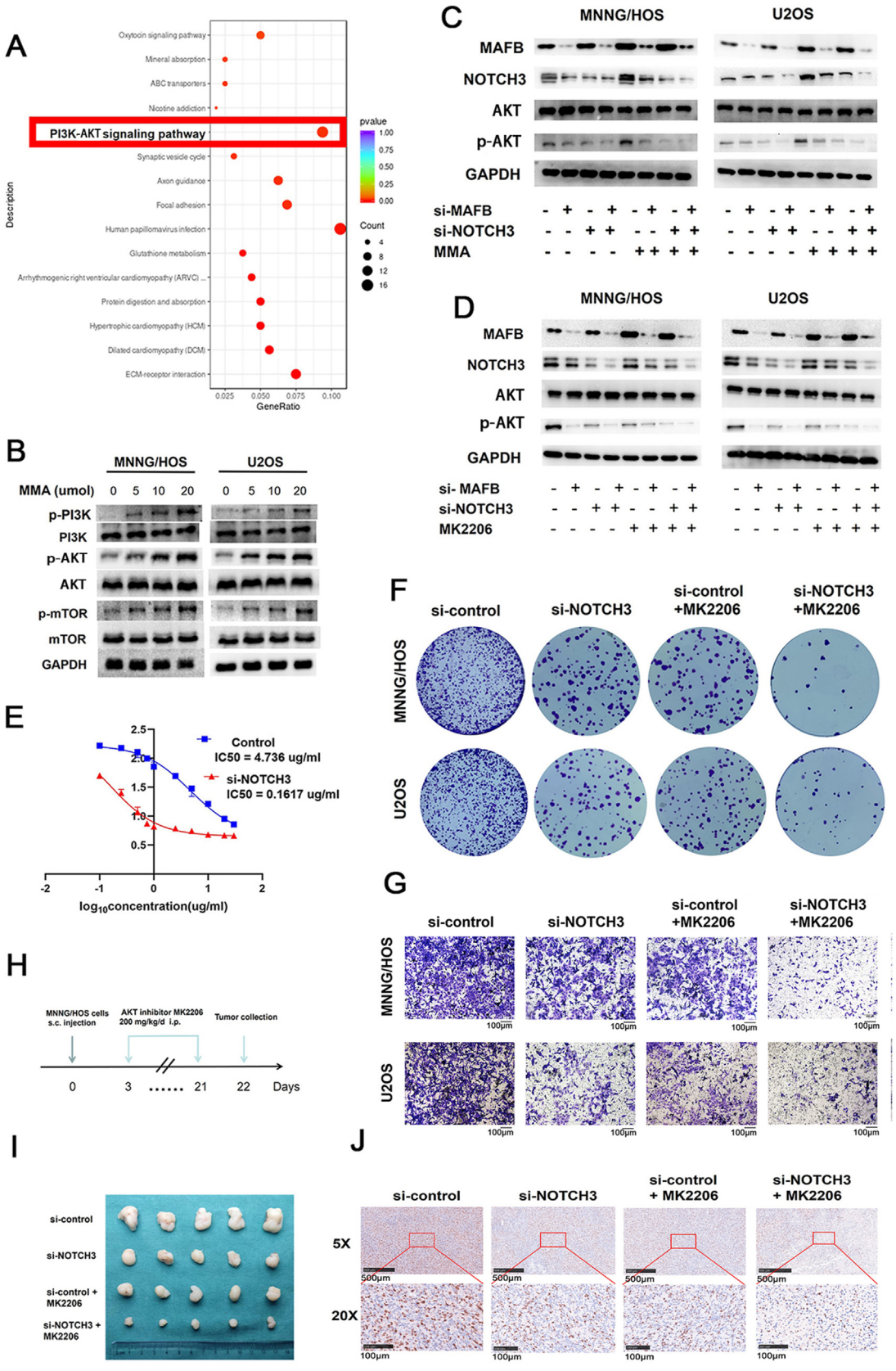

Figure 5 Activation of the *PI3K-AKT* pathway by the *MAFB-NOTCH3* axis promotes osteosarcoma proliferation. **(A)** Dot plot of the KEGG enrichment pathways in the MMA treatment group. **(B)** The expression of components of the *PI3K-AKT-mTOR* pathway was

Discussion

Cellular senescence is an important protective mechanism for maintaining the stability of the internal environment of tissues.[21] An increasing body of evidence shows that senescent cells stimulate tumor development and malignant progression via various processes.[6,7] Recent studies have shown that senescent cells can accelerate tumor progression by remodeling the tumor microenvironment and cellular transcription patterns, which are mediated by specific metabolites.[22] Because it primarily occurs in adolescents and young adults, osteosarcoma is one of the most common pediatric tumors.[23] However, surprisingly, the number of elderly patients is increasing, and the elderly population represents the second peak of osteosarcoma incidence.[24] The mechanism underlying osteosarcoma development in elderly patients is intriguing, and a connection between tumor progression and cellular senescence may be considered.

Endogenous metabolic by-products are critical regulators in cancer development and carcinogenicity.[25] A new study has revealed that the accumulation of MMA in the serum of older individuals plays a central role in tumor aggressiveness, thus contributing to tumor progression, which represents a novel relationship between aging and cancer.[8] However, to date, no study has been conducted on the specific functions of MMA in other cancers.

MAFB, a member of the *MAF* transcription factor family, contains basic leucine zipper domains that bind to specific DNA elements.[16] *MAFB* regulate cell differentiation[14] and the pattern of tissue-specific gene expression[15] in various tissues and participate in human tumor genesis and development.[14] However, the role of *MAFB* in osteosarcoma has rarely been reported.

The *NOTCH* pathway is not only involved in normal embryonic development[26] but also plays an important role in the development of cancers.[27] The *NOTCH3* gene, a member of the *NOTCH* family, encodes a single-pass transmembrane heterodimer receptor protein.[28] In typical *NOTCH3* signaling, *NOTCH3* intracellular domain (NICD3) moves to the nucleus, where it binds to CSL and activates the transcription of *Hey* and *Hes1*.[29] It has been proved that *NOTCH3* dysfunction could widely affect cancer aggressiveness and chemotherapy resistance.[30] Multivariate analysis revealed that *NOTCH3* was an independent prognostic factor for osteosarcoma.[31] Findings from a recent study in T-cell acute lymphoblastic leukemia confirmed that *MAFB* enhances carcinogenicity via up-regulating *NOTCH1* signaling.[32] However, to date, no study has been conducted on the specific relationship between *MAFB* and *NOTCH3*.

Conclusions

Considering that osteosarcoma has the second peak incidence in the elderly,[3,4] we evaluated findings from the existing study on the relationship between MMA levels and "old" age.[8] Thus, we hypothesized that the systematic accumulation of MMA caused by cellular senescence would accelerate osteosarcoma progression. Interestingly, our findings showed that osteosarcoma cells can modulate their transcription pattern by directly using the metabolic components produced in response to cellular senescence. Our data showed that the significant accumulation of MMA in elderly patients endowed osteosarcoma cells with proliferative properties. The expression of *MAFB* was excessively up-regulated in osteosarcoma specimens and was further enhanced in response to MMA accumulation as the patient aged. Specifically, we confirmed that *MAFB* up-regulated *NOTCH3* at the transcriptional level to promote the proliferation of osteosarcoma, which relies on the activation of the *PI3K-AKT* pathway. Moreover, the down-regulation of the *MAFB-NOTCH3* axis could increase the sensitivity and effect of *AKT* inhibitors in osteosarcoma by significantly inhibiting *AKT* phosphorylation. In conclusion, we first confirmed that *MAFB* is a novel age-dependent biomarker for osteosarcoma and our data showed that targeting the *MAFB-NOTCH3* axis in combination with *AKT* inhibitor administration could serve as a novel therapeutic strategy in elderly patients with osteosarcoma that can be explored in experimental and clinical trials.

Author contributions

Zhenhao Zhang, Doudou Jing, and Baijun Xuan performed the experiments. Doudou Jing and Wei Wu collected the data. Zhenhao Zhang and Wei Wu wrote the paper and analyzed the data. Zengwu Shao and Zhicai Zhang revised the manuscript. All authors read and approved the final manuscript.

confirmed by Western blot analysis. MNNG/HOS and U2OS cells were treated with 0, 5, 10, and 20 mmol/L MMA. **(C)** The expression of *MAFB*, *NOTCH3*, *AKT*, and *p-AKT* was detected by Western blot analysis. MNNG/HOS and U2OS cells treated with or without MMA were transfected with si-*MAFB* or si-*NOTCH3*, respectively. **(D)** The expression of *MAFB*, *NOTCH3*, *AKT*, and *p-AKT* was detected by Western blot analysis. MNNG/HOS and U2OS cells treated with or without MKK2206 were transfected with si-*MAFB* or si-*NOTCH3*, respectively. **(E)** The sensitivity of MNNG/HOS cells to MK2206 was detected in the CCK8 assay and measured in terms of the IC_{50} value. MNNG/HOS cells treated with MK2206 at different concentrations were transfected with si-*NOTCH3* or si-control. Data were presented as mean $\pm$ SD of three replicates. The IC_{50} of the si-control group was 4.736 μg/mL. The IC_{50} of the si-*NOTCH3* group was 0.1617 μg/mL. **(F)** Cell proliferation was detected in the colony-forming assay. Implanted MNNG/HOS cells were transfected with si-*NOTCH3* or si-Control; cells were treated with MK2206 or PBS. **(G)** The cell migration potential was detected in the Transwell assay. The groups were formed as mentioned above. **(H)** Flow diagram for the xenograft assay in nude mice. **(I)** Results of the xenograft assay in nude mice. Implanted MMNNG/HOS cells were transfected with si-*NOTCH3* or si-Control; cells were treated with MK2206 or PBS. $n = 5$. **(J)** The tumor tissue acquired from the nude mice xenograft assay was subjected to immunohistochemistry for Ki-67 staining. The groups were formed as mentioned above. $n = 5$.

Data availability

Please contact the corresponding author Wei Wu (waynewu@hust.edu.cn) for data requests.

Conflict of interests

There was no potential conflict of interests disclosed.

Funding

This work was supported by grants from the National Natural Science Foundation of China (No. 82072979).

Acknowledgements

We would like to express our gratitude to all those who helped us during the writing of this paper. We gratefully acknowledge the help of my supervisor, Prof. Zengwu Shao, who offered us valuable suggestions for academic studies. We thank Bullet Edits Limited for the linguistic editing and proofreading of the manuscript.

Appendix A. Supplementary data

Supplementary data to this article can be found online at https://doi.org/10.1016/j.gendis.2023.02.028.

References

1. Rainusso N, Wang LL, Yustein JT. The adolescent and young adult with cancer: state of the art - bone tumors. *Curr Oncol Rep*. 2013;15(4):296—307.
2. Nishida Y, Isu K, Ueda T, et al. Osteosarcoma in the elderly over 60 years: a multicenter study by the Japanese musculoskeletal oncology group. *J Surg Oncol*. 2009;100(1):48—54.
3. Hayakawa K, Matsumoto S, Ae K, et al. Definitive surgery of primary lesion should be prioritized over preoperative chemotherapy to treat high-grade osteosarcoma in patients aged 41-65 years. *J Orthop Traumatol*. 2020;21:13.
4. Imura Y, Takenaka S, Kakunaga S, et al. Survival analysis of elderly patients with osteosarcoma. *Int Orthop*. 2019;43(7):1741—1747.
5. Gill J, Gorlick R. Advancing therapy for osteosarcoma. *Nat Rev Clin Oncol*. 2021;18(10):609—624.
6. Kowald A, Passos JF, Kirkwood TBL. On the evolution of cellular senescence. *Aging Cell*. 2020;19(12):e13270.
7. Wang B, Kohli J, Demaria M. Senescent cells in cancer therapy: friends or foes? *Trends Cancer*. 2020;6(10):838—857.
8. Gomes AP, Ilter D, Low V, et al. Age-induced accumulation of methylmalonic acid promotes tumour progression. *Nature*. 2020;585(7824):283—287.
9. Lai Y, Tang F, Huang Y, et al. The tumour microenvironment and metabolism in renal cell carcinoma targeted or immune therapy. *J Cell Physiol*. 2021;236(3):1616—1627.
10. Chandler RJ, Venditti CP. Genetic and genomic systems to study methylmalonic acidemia. *Mol Genet Metabol*. 2005;86(1—2):34—43.
11. Pai ELL, Vogt D, Clemente-Perez A, et al. *Mafb* and *c-maf* have prenatal compensatory and postnatal antagonistic roles in cortical interneuron fate and function. *Cell Rep*. 2019;26(5):1157—1173.
12. Blank V, Andrews NC. The Maf transcription factors: regulators of differentiation. *Trends Biochem Sci*. 1997;22(11):437—441.
13. Nishizawa M, Kataoka K, Goto N, et al. V-Maf, a viral oncogene that encodes a "leucine zipper" motif. *Proc Natl Acad Sci U S A*. 1989;86(20):7711—7715.
14. Eychène A, Rocques N, Pouponnot C. A new MAFia in cancer. *Nat Rev Cancer*. 2008;8(9):683—693.
15. Kataoka K. Multiple mechanisms and functions of maf transcription factors in the regulation of tissue-specific genes. *J Biochem*. 2007;141(6):775—781.
16. Li Y, Min D, Wang K, et al. microRNA-152 inhibits cell proliferation, migration and invasion by directly targeting MAFB in nasopharyngeal carcinoma. *Mol Med Rep*. 2017;15(2):948—956.
17. Boersma-Vreugdenhil GR, Kuipers J, Van Stralen E, et al. The recurrent translocation t(14;20)(q32;q12) in multiple myeloma results in aberrant expression of MAFB: a molecular and genetic analysis of the chromosomal breakpoint. *Br J Haematol*. 2004;126(3):355—363.
18. Yadav MK, Inoue Y, Nakane-Otani A, et al. Transcription factor MafB is a marker of tumor-associated macrophages in both mouse and humans. *Biochem Biophys Res Commun*. 2020;521(3):590—595.
19. Martínez-Reyes I, Chandel NS. Cancer metabolism: looking forward. *Nat Rev Cancer*. 2021;21(10):669—680.
20. Ediriweera MK, Tennekoon KH, Samarakoon SR. Role of the PI3K/AKT/mTOR signaling pathway in ovarian cancer: biological and therapeutic significance. *Semin Cancer Biol*. 2019;59:147—160.
21. Hanahan D, Weinberg R. Hallmarks of cancer: the next generation. *Cell*. 2011;144(5):646—674.
22. Birch J, Gil J. Senescence and the SASP: many therapeutic avenues. *Genes Dev*. 2020;34(23—24):1565—1576.
23. Kent PM, Ording J, Dabrowski E, et al. Introduction: malignant primary bone tumors in children and young adults. *Curr Probl Cancer*. 2013;37(4):160—166.
24. Mirabello L, Troisi RJ, Savage SA. Osteosarcoma incidence and survival rates from 1973 to 2004: data from the surveillance, epidemiology, and end results program. *Cancer*. 2009;115(7):1531—1543.
25. Sun L, Suo C, Li ST, et al. Metabolic reprogramming for cancer cells and their microenvironment: beyond the Warburg Effect. *Biochim Biophys Acta Rev Cancer*. 2018;1870(1):51—66.
26. Gama-Norton L, Ferrando E, Ruiz-Herguido C, et al. Notch signal strength controls cell fate in the haemogenic endothelium. *Nat Commun*. 2015;6:8510.
27. Meurette O, Mehlen P. Notch signaling in the tumor microenvironment. *Cancer Cell*. 2018;34(4):536—548.
28. Lardelli M, Dahlstrand J, Lendahl U. The novel *Notch* homologue mouse *Notch 3* lacks specific epidermal growth factor-repeats and is expressed in proliferating neuroepithelium. *Mech Dev*. 1994;46(2):123—136.
29. Hosseini-Alghaderi S, Baron M. Notch 3 in development, health and disease. *Biomolecules*. 2020;10(3):485.
30. Aburjania Z, Jang S, Whitt J, et al. The role of Notch 3 in cancer. *Oncol*. 2018;23(8):900—911.
31. Tang XF, Cao Y, Peng DB, et al. Overexpression of Notch 3 is associated with metastasis and poor prognosis in osteosarcoma patients. *Cancer Manag Res*. 2019;11:547—559.
32. Pajcini KV, Xu L, Shao L, et al. MAFB enhances oncogenic Notch signaling in T cell acute lymphoblastic leukemia. *Sci Signal*. 2017;10(505):eaam6846.